

Host Focal Adhesion Protein Domains That Bind to The Translocated Intimin Receptor (Tir) of Enteropathogenic *Escherichia coli* (EPEC)

Lily Huang, Balraj Mittal, Joseph W. Sanger, and Jean M. Sanger*

Department of Cell and Developmental Biology, University of Pennsylvania School of Medicine, Philadelphia

Enteropathogenic *Escherichia coli* (EPEC) attach to the plasma membrane of infected host cells and induce diarrhea in a variety of farm animals as well in humans. These bacteria inject a three-domain protein receptor, Tir (translocated intimin receptor), that is subsequently inserted into the plasma membrane. EPEC induce the host cell to form membrane-covered actin-rich columns called pedestals. Focal adhesion constituents, alpha-actinin, talin, and vinculin, are localized along the length of the pedestals and we have previously reported they bind the two cytoplasmic domains of Tir, (Tir I and Tir III) [Freeman et al., 2000: *Cell Motil. Cytoskeleton* 47:307–318]. In the present study, various constructs were made expressing different regions of these three focal adhesion proteins to determine which domains of the proteins bound Tir I. Three different assays were used to detect Tir I/host protein domain interactions. In co-precipitation assays, His-Tir I bound to the 27-kDa region of alpha-actinin; to four different domains of talin; and to the N-terminal domain of the vinculin head and the vinculin tail domain. A yeast two-hybrid analysis of Tir I and the various focal adhesion fusion proteins revealed a region near the C-terminus of talin was the only domain to interact with Tir I. Finally, to assess direct binding interactions, biotinylated Tir I was used in overlay assays and confirmed the binding of Tir I with the 27-kDa region of alpha-actinin, the four regions of talin, and the vinculin tail. These binding interactions between hostfocal adhesion proteins and EPEC Tir may facilitate the adhesion of EPEC to the host cell surface. *Cell Motil. Cytoskeleton* 52:255–265, 2002.

© 2002 Wiley-Liss, Inc.

Key words: alpha-actinin; talin; vinculin; pathogens; pedestals.

INTRODUCTION

The natural habitat of *Escherichia coli* (*E. coli*) is the intestine of animals where most *E. coli* strains exist in a mutually beneficial interaction with their hosts. A group of pathogenic *E. coli*, however, have evolved that colonize the intestinal mucosa where they adhere tightly to the epithelial cells and cause diarrhea in animals and man [Levine, 1987; Marches et al., 2000]. Enteropathogenic *E. coli* (EPEC) are a significant cause of diarrhea in neonatal calves as well as in post-weaning pigs and rabbits, and possibly in chicks [Fukui et al., 1995; Marches et al., 2000]. It is also a leading cause of diarrhea in infants in developing countries [Nataro and Kaper, 1998].

EPEC are members of a group of bacteria that attach to host cells and induce the formation of an actin-

rich column called a pedestal [Celli et al., 2000; Goosney et al., 2000b]. The process requires that EPEC secrete a

Dr. Balraj Mittal was a Visiting Scientist at the University of Pennsylvania School of Medicine. His current address is Sanjay Gandhi Postgraduate Institute of Medical Sciences, Lucknow, India.

Contract Grant Sponsor: USDA.

*Correspondence to: Dr. Jean M. Sanger, Department of Cell and Developmental Biology, University of Pennsylvania School of Medicine, 421 Curie Boulevard, BRB II/III, Philadelphia, PA 19104-6058. E-mail: sangerjm@mail.med.upenn.edu

Received 15 January 2002; Accepted 25 March 2002

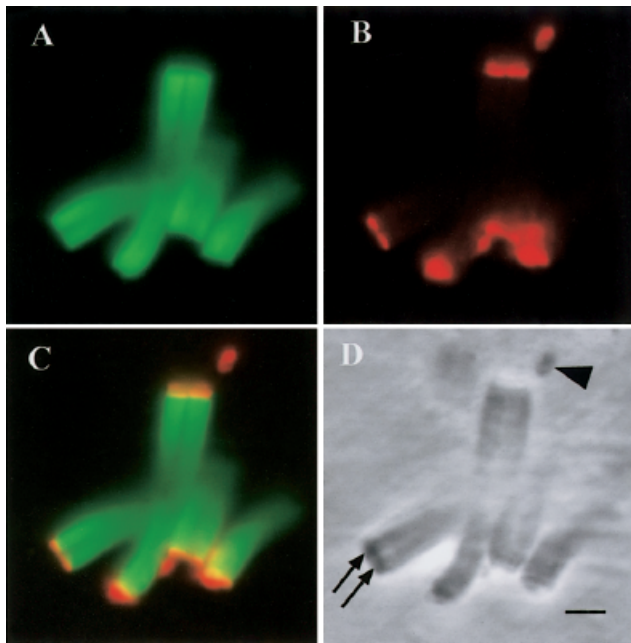


Fig. 1. Epifluorescence and phase-contrast images of pedestals induced by EPEC on PtK2 cells. **A:** Actin was stained with FITC-phalloidin and is shown in green. **B:** The same infected cell was stained with an antibody directed against the first cytoplasmic domain of Tir (Tir I) and a rhodamine-labeled secondary antibody shown in red. **C:** Merged images of A and B show orange and yellow where there is colocalization of actin and Tir I at the tip of the pedestal. **D:** Phase-contrast image with two of the attached EPEC marked by arrows. The pedestals are over 10 μm long and curved so that the focal plane is not always parallel to the long axis of the pedestal at the tip where it binds EPEC. This sometimes results in red Tir I signal that appears to extend beyond the actin filaments in the pedestals. The arrowhead in D indicates the position of a bacterium on top of a small pedestal whose actin signal is not visible. Scale = 5 μm .

protein receptor that inserts into the plasma membrane of the host cell. This receptor, translocated intimin receptor (Tir), is positioned with the first and third domain internal to the host cytoplasm separated by the external second domain that binds the bacterial surface protein, intimin [de Grado et al., 1999; Luo et al., 2000; Vallance and Finlay, 2000]. Tir is thus positioned at the top of the pedestal that is filled with actin filaments (Fig. 1). This attachment is believed to give EPEC and other bacteria of this class, e.g., Enterohemorrhagic *E. coli* (EHEC) and *Helicobacter pylori*, an ecological advantage in the gastrointestinal (GI) tract where many other strains of bacteria live [Hooper et al., 1998; Savage, 1977].

EPEC are found primarily in the small intestine where their attachment to the surfaces of the enterocytes induces the loss of the microvilli, followed by the reorganization of the surface actin into raised pedestals. Thus, these microbes are referred to as attaching and effacing (A/E) bacteria. While exact virulence mechanisms remain poorly understood, pedestal formation ap-

pears important for the virulence of these bacteria. Mutants of EPEC that attach but do not induce the formation of pedestals have a decreased ability to induce diarrhea in student volunteers [Donnenberg et al., 1993]. Marches et al. [2000] generated two mutants of rabbit EPEC (REPEC) that lacked either Tir or intimin. Neither mutant was able to induce pedestal formation or induce any clinical signs of disease. In contrast, infection with the parental strain of REPEC caused the death of 90% of the infected, weaned rabbits. Clearly, an understanding of the molecular mechanisms involved in pedestal formation will allow important insights into this group of A/E infectious bacteria.

A large group of proteins have been detected along with actin in the pedestals of EPEC [Freeman et al., 2000; Goosney et al., 2001; Gruenheid et al., 2001; Sanger et al., 1996]. Structurally, the pedestals appear to have properties of both microvilli and focal adhesions [Freeman et al., 2000]. Pedestal shape, the distribution of villin and ERM proteins along the length of the actin filaments, and myosin II and tropomyosin at the base of the filament bundles suggest resemblances to microvilli [Freeman et al., 2000; Sanger et al., 1996]. Characteristics similar to focal adhesion properties include the attachment site of the bacteria at the tip of the pedestal and the congregation of several focal adhesion proteins, e.g., alpha-actinin, talin, and vinculin, decorating the length of the pedestal [Freeman et al., 2000; Goosney et al., 2001]. The ability of focal adhesion proteins and Tir to interact may assist EPEC in remaining attached during peristalsis of the GI tract.

There have been conflicting reports concerning the binding of alpha-actinin, talin and vinculin to the cytoplasmic domains of Tir [Cantarelli et al., 2001; Freeman et al., 2000; Goosney et al., 2000]. In this report, we have used three different protein-binding assays to determine which domains of alpha-actinin, talin and vinculin bind the first cytoplasmic domain of Tir (Tir I). Finally, we suggest these focal adhesion proteins compete in their interactions with TirI in vivo as the N-terminus of talin was able to displace a fraction of the vinculin tail fusion protein that was bound to Tir I. Our results support the idea that pedestal attachments to EPEC can be viewed as a focal adhesion with the transmembrane protein Tir, like integrin, linking extracellular molecules (in this case, the bacterial surface protein intimin) to the internal cytoskeleton of the cell [Freeman et al., 2000; Goosney et al., 2001].

MATERIALS AND METHODS

Bacterial Culture, Tissue Culture Cells, and Image Processing

EPEC strain E2348/69 was used to infect PtK2 cells as previously described by Freeman et al. [2000].

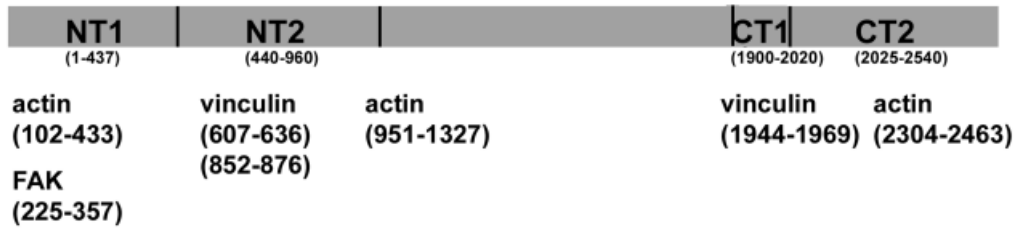
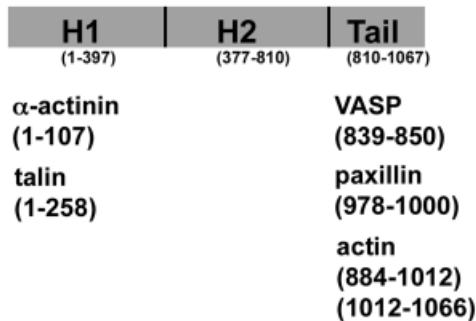
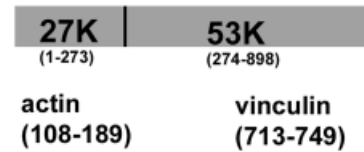
Talin**Vinculin** **α -actinin**

Fig. 2. Domain maps of alpha-actinin, talin, and vinculin. The divisions in each molecule mark the domains constructed for the determination of their interactions with Tir I.

PtK2 cells were cultured and processed for immunofluorescence as reported by Sanger et al. [1996]. Images of the infected cells were taken with a Nikon Diaphot 200 inverted microscope, with Hamamatsu Orca camera and Image Pro software (Phase 3 Imaging Systems, Glen Mills, PA) and assembled with Adobe (San Jose, CA) Photoshop software.

His-Tagged Tir I Construct

The Tir I fusion constructs resulted from cloning a 699-bp polymerase chain reaction (PCR) *Bam*HI/*Hind*III fragment amplified from EPEC genomic DNA into the appropriately digested plasmids: pGEX6p-1 (Amersham Biosciences, Piscataway, NJ) for glutathione *S*-transferase (GST) fusion protein, and pET-28a (Novagen, Madison, WI) for histidine (His) fusion protein. Primers for pGST- Tir I are as described in Freeman et al. [2000]. Primers for His-Tir I were the 5' PCR primer TAG-GATCCG ATG CCT ATT GGT AAC CTT GGT and the 3' primer GACAAGCTT TTT AGG ATC TGA GCG AAC GAT GGA.

Host Protein Fusion Constructs

Expression and cloning of alpha-actinin, talin, and vinculin also employed the pGEX6p-1 fusion system. Figure 2 illustrates the expressed domains of alpha-actinin, talin, and vinculin and the corresponding amino acid sequences.

The 95-kDa alpha-actinin molecule can be divided into two main domains (Fig. 2): the N-terminal region, amino acids 1 to 273, contains the actin-binding region of alpha-actinin, and is termed 27K in reference to its size. pGST-27K resulted from cloning an 819-bp PCR-amplified *Eco*RI/*Xho*I fragment, pGST-27K, with the 5' PCR primer GCCGAATTC ATG AAC AGC ATG AAC CAG ATA and the 3' primer TTA CTG CAG ACA GAT CCG GTT TGC TGC AGT. The carboxyl terminus of alpha-actinin, amino acids 274 to 898, contains the spectrin repeats and the integrin-binding domain and is designated 53K. pGST-53K expresses alpha-actinin amino acids 274 to 898 and results from cloning an 1,875-bp PCR *Eco*RI/*Xho*I amplified fragment, using the 5' PCR primer GCCGAATTC AAG GTG CTT GCT GTG AAT CAA and the 3' primer GTCTCGAG TCA GAG ATC GCT CTC TCC ATA.

Talin, a 225-kDa molecule with multiple binding sites for other interacting proteins, including three actin- and three vinculin-binding domains (Fig. 2). We made four different domain constructs of this molecule. The first construct in pGST-Talin-NT1, expresses talin amino acids 1 to 437 and encodes an actin binding domain as well as FAK, layilin, and beta-integrin binding domains. pGST-Talin-NT1 results from cloning an 1,311-bp PCR *Eco*RI/*Xho*I amplified fragment, using the 5' PCR primer CGGAATTC ATG GTT GCG CTT TCG GCT GAA G and the 3' PCR primer TTCTCGAGTCA TTT CCC CAC

TCG GTT GTA C. The second construct, pGST-Talin-NT2, expresses amino acids 440 to 960 and encodes two vinculin-binding domains. pGST-Talin-NT2 results from cloning a 1,563-bp PCR amplified *EcoRI/XhoI* fragment, using the 5' PCR primer TTGAATTC GTG GAG CAC GGC TCT GTG GCT C and the 3' PCR primer TTCTC-GAGTCA TGC CAC GGC CTT ACA GCT C. The third construct, pGST-Talin-CT1, expresses talin amino acids 1,900 to 2,020 and encodes an actin binding domain and one vinculin-binding domain. pGST-Talin-CT1 results from cloning a 363-bp PCR amplified *EcoRI/XhoI* fragment, using the 5' PCR primer ATGAATTC AAG CCT GCA GCT GTG GCT GCT G and the 3' PCR primer TCTCGAG TAA GAT ACC CTC CCG GTG GTC AGC AAA. The fourth construct, pGST-Talin-CT2, expresses talin amino acids 2,025 to 2,540 and encodes an actin-binding domain. pGST-Talin-CT2 results from cloning a 1,548-bp PCR amplified *EcoRI/XhoI* fragment, GST-Talin-CT2, with the 5' PCR primer GGAATTC CTT GTG GAG GAC ACC AAG GTC CTA and the 3' PCR primer GTCTCGAG TTA GTG CTC GTC TCG AAG CTC T.

Vinculin, a 130-kDa protein, is composed of a large head region and a small tail region. The molecule was divided into three domains for the constructs we assembled: two head regions and one tail region (Fig. 2). The first head construct in pGST-Vinculin-H1 encodes amino acids 1 to 397 and includes a talin- and an alpha-actinin-binding region. pGST-Vinculin-H1 results from cloning a 1,191-bp PCR amplified *Sall/NotI* fragment, using the 5' PCR primer TGTCGACTT ATG CCC GTC TTC CAC ACG CGC and the 3' primer TAGCGGCCGCTT ATC CGC AAG CCA GTT CTG. The second head region construct, pGST-Vinculin-H2, encodes amino acids 377 to 810 and contains no known binding domains. pGST-Vinculin-H2 results from cloning a 1,302-bp PCR *Sall/NotI* fragment using the 5' PCR primer CGTCGACGC ATG ACA AAC TCT AAG CAG GCT and the 3' primer TAGCGGCCGCTG ATC AGA GAT ATT TCC TGC. The third vinculin construct, the tail domain, pGST-Vinculin-Tail, encodes amino acids 810 to 1,067. This region includes binding sites for actin, paxillin, and VASP. pGST-Vinculin-Tail results from cloning a 774-bp PCR amplified *Sall/NotI* fragment, using the 5' PCR primer TGTCGACGC GAT CCT GGT TTG CAG AAG AGT and the 3' primer TAGCGGCCGCTA TTA CTG ATA CCA TGG GGT.

Expression of Fusion Proteins

All GST-fusion constructs were transformed into *E. coli* DH5 α (Life Technologies, Inc., Grand Island, NY), and sequences were confirmed (Napcore, The Children's Hospital of Philadelphia, Philadelphia, PA). GST-fusion proteins were expressed in *E. coli* BL-21(DE3)pLysS and induced with IPTG. GST-Tir I was purified as previously reported [Freeman et al., 2000]. A portion of the

purified GST-Tir I was proteolysed with Precision protease (Amersham Pharmacia Biotech, Piscataway, NJ) and the manufacturer's recommendations to isolate Tir I free from GST. In some assays, purified GST-host-protein domains were also proteolysed with Precision protease. His-Tir I was purified with the HisTrap purification kit (Amersham Biosciences, Piscataway, NJ), following the manufacturer's instructions.

Yeast-2 Hybrid Analysis

Two hybrid interactions were assessed using a commercially available yeast two-hybrid kit (Hybrid Hunter), purchased from Invitrogen Corporation (Carlsbad, CA). Tir I cDNA encoding amino acids 1–233 was cloned into the pHybLex/Zeo plasmid (bait) and each cDNA encoding three different fragments of alpha-actinin (amino acids 1–245, 273–746 [spectrin repeat domains, SR], 746–898), four fragments of talin (amino acids 1–437, 440–959, 1,898–2,019, 2,024–2,542), and three fragments of vinculin (amino acids 1–397, 376–811, 809–1,067) were cloned individually into pYESTrp2 plasmid (prey). To construct the Tir I bait, pHybLex/Zeo-Tir I, the 5' PCR primer: GGG CTG AAT TCA TGC CTA TTG GTA ACC TTG and the 3' primer: GAT TCG TCG ACC TAT TTA GGA TCT GAG CGA ACG were used to amplify and clone an *EcoR I/Sal I* xxx bp fragment into the pHybLex/Zeo bait vector.

pYESTrp2-talin-CT2, encoding amino acids 2,024–2,542, was generated by cloning a 1,553-bp PCR *EcoR I/Xho I* amplified product (5' primer: GGA ATT CTT GTG GAG GAC ACC AAG GTC CTA; 3' primer: TC TCG AGT TTA GTG CTC GTC TCG AAG CTC) into pYESTrp2 prey vector. The other talin domain baits were generated using the following primers and restriction enzymes (*EcoR I/Xho I* site): pYESTrp2-talin-nt1 (amino acids 1–437), (5' primer: C AGA ATT CTG ATG GTT GCG CTT TCG CTG AAG; 3' primer: TTC TCG AGG GTT GTA CTG CTG CTG AAG GAC); pYESTrp2-talin-nt2 (amino acids 273–746) (5' primer: A TGA ATT CTA GTG GAG CAC GGC TCT GTG GCT C; 3' primer: TTC TCG AGG TGC CAC GGC CTT ACA GCT CTG); pYESTrp2-talin-ct1 (amino acids 1,898–2,019) (5' primer: T TGA ATT CAA GCC AAG CCT GCA GCT GTG GCT; 3' primer: TC TCG AGA GAT ACC CTC CCG GTG GTC AGC AAA).

The alpha-actinin domain baits were generated using the following primers and restriction enzymes (*Hind III/Xho I* site): pYESTrp2-alpha-actinin-nt, (amino acids 1–245) (5' primer: G GGG AAG CTT ATG AAC AGC ATG AAC CAG; 3' primer: TTT TCT CGA GCT CAT CAG GTT TGG GAG TG); pYESTrp2-alpha-actinin-sr, (amino acids 273–746) (5' primer: GT AAG CTT AAG GTG CTT GCT GTG AAT CAA G; 3' primer: TT C TCG AGG GAGGAT CTG AGT CTC AAC CTC); pYESTrp2-alpha-actinin-ct, (amino acids 746–898) (5'

primer: GT AAG CTT ACA AGA GAT GCC AAG GGT ATC; 3' primer: GT C TCG AGG TCA GAG ATC GCT CTC TCC ATA).

The vinculin domain baits were constructed using the following primers and restriction enzymes (*Hind* III/*Xho* I site): pYESTrp2-vinculin-h1 (amino acids 1–397) (5' primer: G GAA AAG CTT ATG CCC GTC TTC CAC ACG; 3' primer: TTT GCT CGA GCT AAT CCG CAA GCC AGT TCT G); pYESTrp2-vinculin-h2 (amino acids 376–811), (5' primer: G GGG AAG CTT ATG ACA AAC TCT AAG CAG; 3' primer: CCG GCT CGA GCT AAG GAT CAG AGA TAT TTC CTG) pYESTrp2-vinculin-tail (amino acids 809–1,067), (5' primer: G GAA AAG CTT GAT CCT GGT TTG CAG AAG AGT; 3' primer: CCG GCT CGA GCT TTA CTG ATA CCA TGG GGT).

The yeast host strain L40 was sequentially transformed with pHybLex/Zeo-Tir I bait and one of the following prey plasmids: pYESTrp2-alpha-actinin-nt, pYESTrp2-alpha-actinin-sr, pYESTrp2-alpha-actinin-ct, pYESTrp2-talin-nt1, pYESTrp2-talin-nt2, pYESTrp2-talin-ct1, pYESTrp2-talin-ct2, pYESTrp2-vinculin-h1, pYESTrp2-vinculin-h2 or pYESTrp2-vinculin-tail.

To detect positive reactions of the bait and prey plasmids, we used the colony-lift assay described in a Clontech protocol (Yeast Protocols Handbook, Protocol PT3024-1, Version PR 03065; Clontech, Palo Alto, CA). Briefly, filter paper was placed on the surface of a plate of freshly plated yeast colonies, each colony about 1 to 3 mm in diameter. The filter paper was marked for orientation and pressed onto the colonies of yeast. The filter paper was then placed in a small amount of liquid nitrogen for approximately 10 sec to freeze fracture cells. After equilibrating at room temperature, the filter was placed on another filter paper that had been presoaked in a developing solution containing 5-bromo-4-chloro-3-indoyl-beta-D-galactopyranoside (X-GAL). The filter was incubated at 30°C and checked at 30-min intervals for up to 8 h for the blue color formation.

Antibodies, Co-precipitation, Biotinylated Tir I, and Protein Overlays

Purified alpha-actinin and talin were prepared as previously described [Dold et al., 1994; Hock et al., 1989; Sanger et al., 2000a]. Anti-Tir I polyclonal antibodies [Freeman et al., 2000] were affinity purified with immobilized Tir I. Monoclonal antibody against GST was purchased from Covance-BabCo (Richmond, CA). Biotinylation of Tir I was performed using BioTAG and manufacturer's recommendations (Sigma, St. Louis, MO). In biotinylation assays, purified host protein domains cleaved from GST were run on gels, transferred to nitrocellulose membranes and incubated with Tir I-bi-

otin. Biotin signal was detected with Extravidin peroxidase (Sigma) and chemiluminescence.

Co-precipitation assays used purified His-Tir I purified by the HisTrap purification kit (Amersham Biosciences, Piscataway, NJ). Briefly, Nickel-NTA histidine-binding resin beads (Novagen, Madison, WI) were incubated with His-Tir I at 4°C for 1 h. To remove unbound His-Tir I, these beads were washed twice with phosphate balanced saline (PBS), twice with 20 mM imidazole, 0.5 M NaCl, 20 mM phosphate, pH 7.4, and twice with PBS. Twenty micrograms of purified GST-host protein fragments were added and the mixture incubated at 4°C for 1 h. The beads were washed four times with a PBS solution containing 0.2 M NaCl and 0.05% triton. The beads and protein complexes were centrifuged and the supernatant discarded. SDS-sample buffer was added to the beads and boiled at 100°C for 5 min. Proteins were separated by SDS-PAGE and transferred to nitrocellulose membranes. The membranes were incubated with anti-GST monoclonal antibodies, secondary horseradish peroxidase conjugated antibody, and visualized with chemiluminescence (Amersham, Piscataway, NJ).

RESULTS

Binding of Alpha-Actinin to Tir I.

There are two reports that the full-length alpha-actinin protein binds to the first cytoplasmic domain of Tir I [Goosney et al., 2000a; Freeman et al., 2000]; although another group was unable to detect binding of Tir to this protein in cell lysates [Cantarelli et al., 2001]. To investigate this further, two constructs were assembled to determine which part(s) of alpha-actinin (Fig. 2) bound to Tir I. Nickel-NTA resin saturated with purified His-Tir I was reacted with purified alpha-actinin GST-27k or GST-53k, and analyzed on Western gels. Anti-GST antibody staining revealed that only the N-terminal region of the alpha-actinin molecule bound Tir I (Fig. 3). To confirm this interaction between the N-terminal region of alpha-actinin and Tir I, purified Tir I was biotinylated and used for overlays of gels of full-length alpha-actinin, and the 27- and 53-K fragments from which the GST tags had been removed by digestion with the Precision protease. Figure 4 shows that the biotinylated Tir I bound the full-length alpha-actinin and the 27-K fragment, but not the 53-K fragment. Thus, two independent methods both demonstrated that only the N-terminal region of alpha-actinin interacts with Tir I.

Binding of Talin to Tir I

Tir has been reported to bind to talin from cell lysates [Cantarelli et al., 2001], and to biochemically purified talin [Freeman et al., 2000]. To determine what

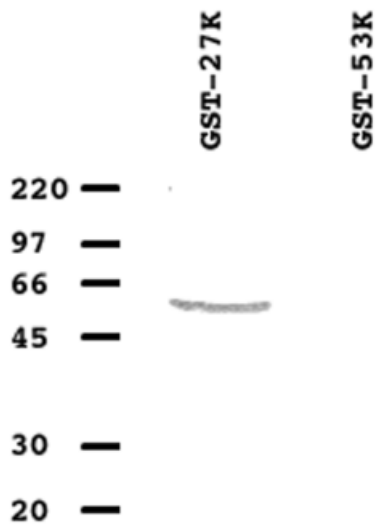


Fig. 3. Western blot demonstrating that Tir I binds to the N-terminal region of alpha-actinin (GST-27 kDa), but not to the 53-kDa region of alpha-actinin (GST-53 kDa). Anti-GST antibody reacts with purified GST-alpha-actinin 27 kDa that coprecipitated with column-purified His-Tir I bound to Ni-NTA resin. The positions of molecular weight markers are indicated on the left.

part of the talin molecule interacted with Tir, we expressed four fusion constructs of the talin molecule (Fig. 2): GST-talin-NT1 (amino acids 1–437); GST-talin-NT2 (amino acids 440–960); GST-talin-CT1 (amino acids 1,900–2,020), and GST-talin-CT2 (amino acids 2,025–2,540), and reacted each with purified His-Tir I that was bound to nickel beads. Western blot analysis with anti-GST-antibodies indicated that three of talin fusion fragments bound Tir I with strong reactions: NT1, NT2, and CT1, with CT2 showing weak reaction (Fig. 5). To confirm these interactions, the GST tag was removed from the talin fusion proteins with the Precision protease, and the fusion proteins were run on a gel. When biotinylated Tir I was used in overlay assays with these GST-less talin fragments, the probe reacted with a strong signal to NT1 and NT2 peptides, but with a weak signal to CT2 and to CT1 (Fig. 6). The probe also bound the full-length, biochemically prepared talin and lower molecular weight products resulting from degradation of native talin (Fig. 6) [Rees et al., 1990]. The Yeast-Two-Hybrid analysis with Tir I as bait revealed that only the Talin-CT2 fragment, and none of the other focal adhesion protein fragments, interacted with the bait Tir I (Fig. 7).

Binding of Vinculin to Tir I

Three GST-fusion proteins encoding three different regions of vinculin (Fig. 2) were generated: GST-vinculin-H1 (amino acids 1–397), GST-vinculin-H2 (amino acids 377–810), and GST-vinculin-tail (amino acids 810–1,067). Western blot analysis indicated that Tir I

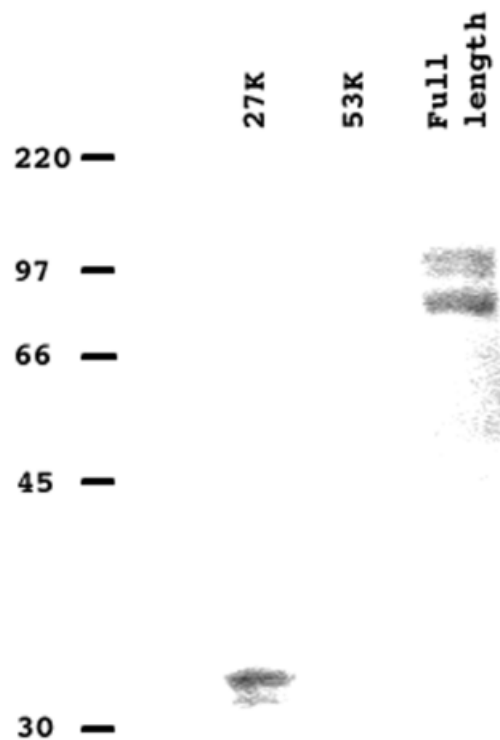


Fig. 4. Extravidin peroxidase reaction of nitrocellulose blot overlaid with Tir I biotin. Biotinylated Tir I binds to the N-terminal domain of alpha-actinin (27 kDa) and to the full length of the alpha-actinin molecule and its proteolytic product. GST-alpha-actinin fragments were column purified and the GST cleaved by PreScission™ Protease. Nitrocellulose blots of gels of the proteins were overlaid with Tir I-biotin and biotin reaction was detected using Extravidin peroxidase conjugate. The positions of molecular weight markers are indicated on the left.

interacted with the H1 (GST-Vinculin-H1) and the tail region (GST-Vinculin-Tail) of the vinculin molecule (Fig. 8). To confirm these interactions, the GST tag was removed from the vinculin fusion proteins with the Precision protease, and the proteins separated and transferred to nitrocellulose. When biotinylated Tir I was added and incubated with the proteins, only the tail region of the vinculin molecule showed binding with Tir I (Fig. 9).

Talin and Vinculin Bind to Different Regions of Tir I

Both GST-talin-NT2 and GST-vinculin-tail fusion proteins interact with Tir I, and biotinylated Tir I binds in a gel overlay assay to these same fusion proteins cleaved free of GST. To determine if Tir I could bind both molecules concurrently, or if prebinding of one protein would inhibit the subsequent binding of the other protein, the talin and vinculin fusion proteins were added sequentially to His-Tir I bound to nickel beads. In separate experiments, the order of addition was varied as was the

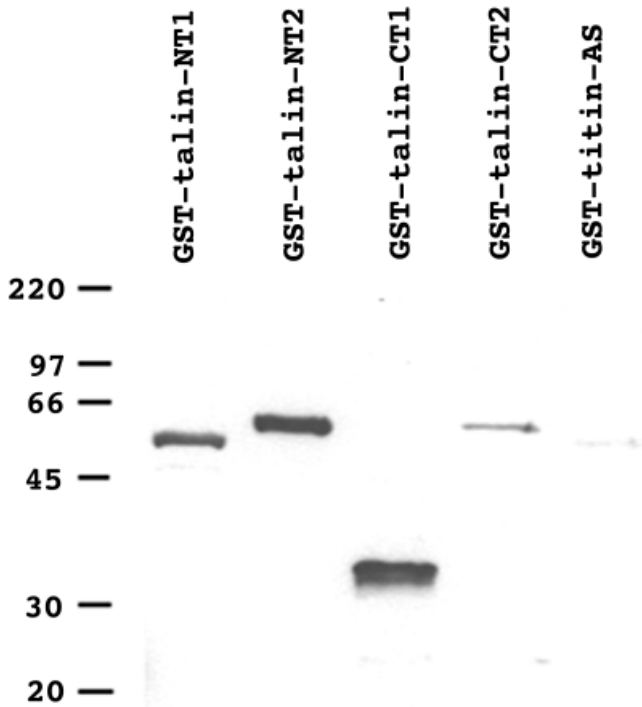


Fig. 5. Western blot demonstrating that Tir I coprecipitates with regions of talin. The first two N-terminal regions (GST-Talin-NT1; GST-Talin-NT2) and the first C-terminal region (GST-Talin-CT1) of talin bind Tir I. The second C-terminal region (GST-Talin-CT2) of talin binds Tir I to a smaller extent. As a negative control, a GST-fragment of titin encoding for a discrete region of the A-band (GST-titin-AS) was also used in this experiment. The positions of molecular weight markers are indicated on the left.

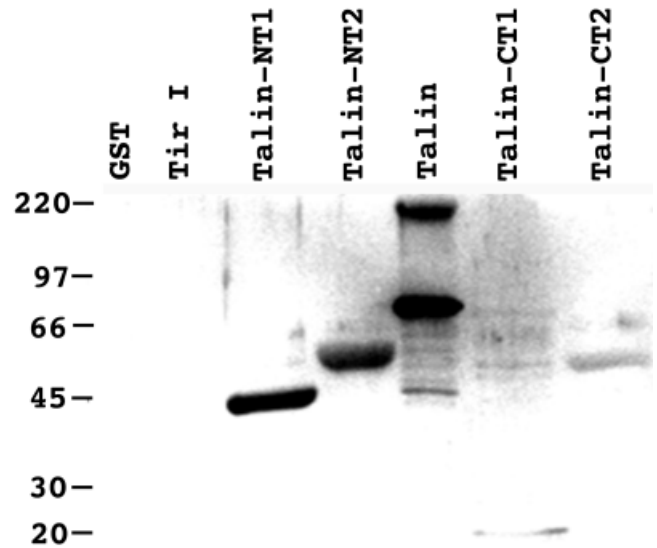


Fig. 6. GST-talin fragments were column purified and the GST cleaved by the PreScission protease before the fragments were run on a gel. Extravidin peroxidase reaction of nitrocellulose blot overlaid with Tir I biotin. Biotinylated Tir I binds strongly to the NT1, NT2 domains of talin and weakly to CT1 and CT2. Full-length talin, prepared from chicken gizzard, binds as do two break-down products in the preparation. The positions of molecular weight markers are indicated on the left. The first lane is GST alone and the second lane is Tir I from which GST was removed as was done for all of the talin fragments.

amount of the first protein added. The results with lower protein concentrations indicated that both proteins bound Tir I concurrently, and that the amount of protein that was bound first did not affect the amount of binding by the secondarily added protein (Fig. 10, lanes 1 to 5). Talin-NT2 binding was saturated at the lower concentrations and the talin was not displaced by vinculin tail protein. The higher concentration of the talin fragment, however, was able to induce some of the bound vinculin tail fragment to be released from Tir I. These experiments suggest that there may be two vinculin tail binding regions in Tir I, one of which binds the talin fragment more avidly than vinculin tail.

DISCUSSION

Of the approximately 10^{14} cells in the human body, only 10% are human eukaryotic cells [Savage, 1977]. The other 90% are almost all bacteria, the vast majority of which reside in the gastrointestinal tract. Normal host flora *E. coli* are outnumbered by at least 400 to 1 by a variety of other bacterial strains [Hooper et al., 1998].



Fig. 7. Yeast Two-Hybrid colony-lift filter assay demonstrating that the only positive interaction was between Tir I and the Talin-CT2 fragment.

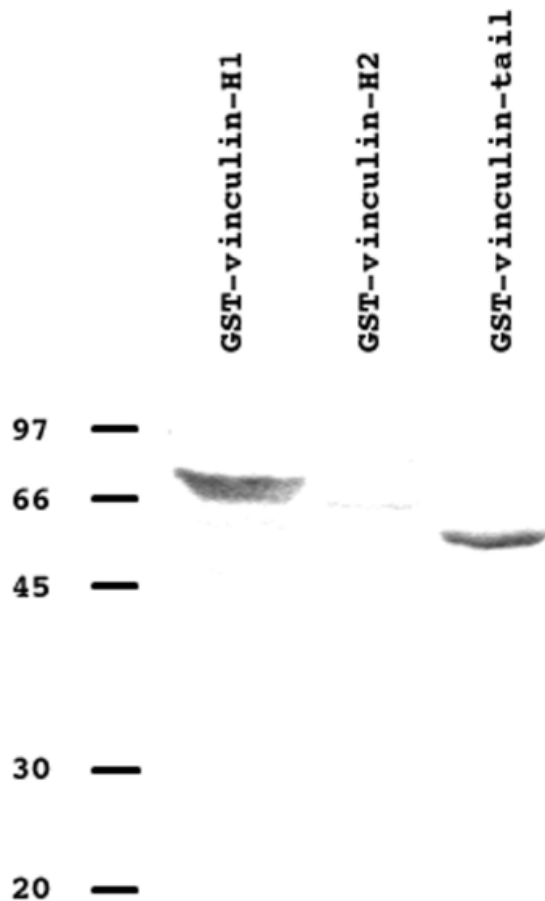


Fig. 8. Western blot demonstrating that Tir I coprecipitates with the N-terminal domain of the vinculin head (GST-Vinculin-H1) and the tail of vinculin. There is no interaction of Tir I with the second part of the vinculin head (GST-Vinculin-H2). The positions of molecular weight markers are indicated on the left.

Unlike almost all the other bacteria in the body, the pathogenic strain of *E. coli*, EPEC, and the foodborne pathogen, *Enterohemorrhagic E. coli* (EHEC), create their niche by attaching to the outer membrane of intestinal cells [DeVinney et al., 1999, 2001]. The actin-rich attachment complexes or pedestals are dynamic structures ranging in length from about 1 to 10 μ . They grow or shorten in length and can undergo undulations and translocate along the surfaces of infected cells [Sanger et al., 1996]. The significance of the pedestals for virulence is not clear, but they may allow the EPEC/EHEC to remain attached to intestinal cells during the host flushing response to rid itself of infectious bacteria [Hecht, 1999], peristalsis of the GI tract, and the intermittent contractions and shortenings of the villi [Neutra, 1988].

The arrangement of Tir in host membranes results in the cytoplasmic localization of two domains: an N-terminal domain of 233 amino acids and a C-terminal domain (amino acids 383–550) with the mid part of the

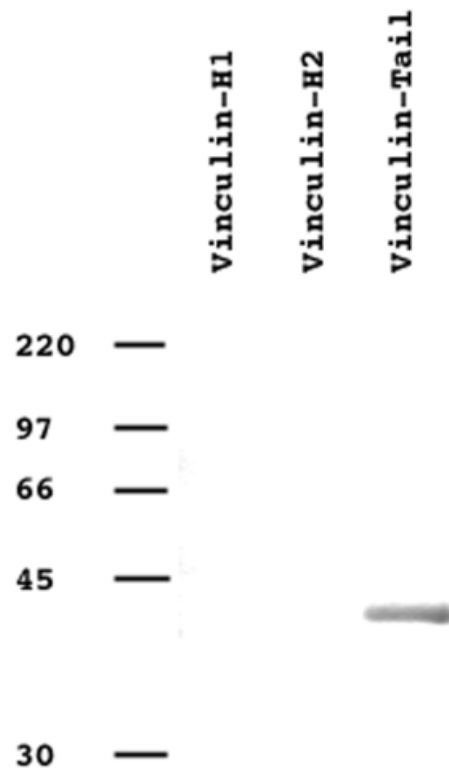


Fig. 9. The GST tags were removed from each of the GST-vinculin fusion proteins by the PreScission protease. Extravidin peroxidase was reacted with a nitrocellulose blot of a gel of the GST-less fusion proteins overlaid with Tir I biotin. Biotinylated Tir I binds to the vinculin tail, but not to either head domain. The positions of molecular weight markers are indicated on the left.

protein (amino acids 260–362) in an extracellular location available to bind intimin [Goosney et al., 2000b]. Several proteins characteristic of focal adhesions [Critchley, 2000] are localized in the pedestals [Freeman et al., 2000; Goosney et al., 2001]. In focal adhesions, these molecules are believed to help cells attach to the substratum by direct and indirect binding to the transmembrane protein, integrin. There is evidence that three focal adhesion proteins, alpha-actinin, talin, and vinculin, bind Tir [Goosney et al., 2000a; Freeman et al., 2000; Cantarelli et al., 2001], although there are discrepancies in the three reports. One group found evidence only for talin binding [Cantarelli et al., 2001]. The second report focused on alpha-actinin, and found binding to Tir I, but not Tir III [Goosney et al., 2000a]. Our group reported binding of the three proteins to both Tir I and Tir III. The different assay methods used in the three studies may be responsible for the disparate results. Our aim in this study was to express segments of the three focal adhesion proteins and use both coprecipitation assays with His-Tir I and gel overlays with biotinylated Tir I to examine binding interactions. Our results indicate that all three

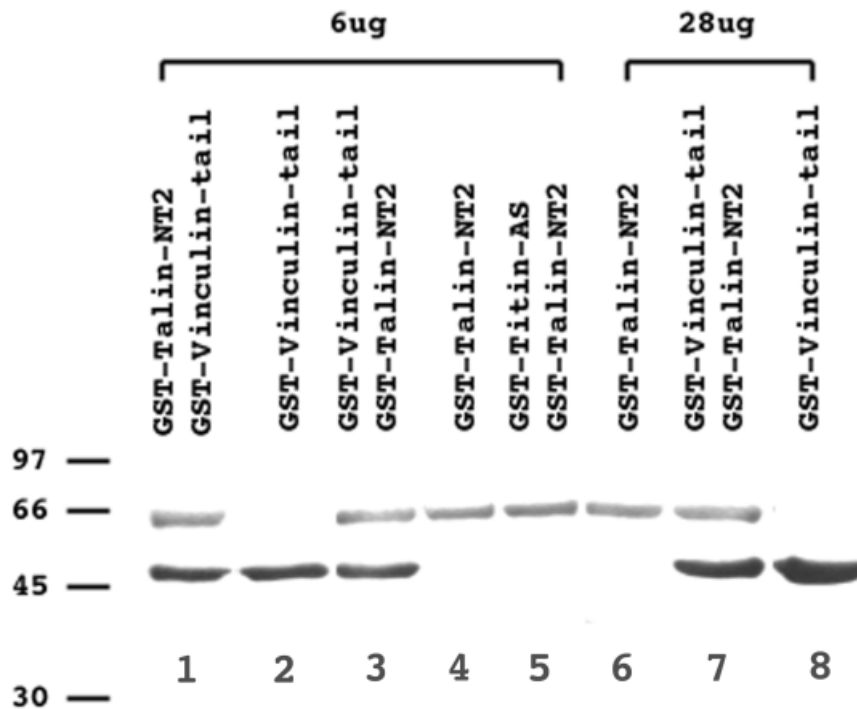


Fig. 10. Western blot of combinations of GST-talin-NT2 and GST-vinculin tail coprecipitating with His-Tir I. Two different amounts, as indicated above the lane markers, of purified GST-talin-NT2 and GST-vinculin-tail fragments were incubated with the His-Tir I coated beads. The samples were run on SDS-PAGE gels and then transferred to a nitrocellulose membrane, which was blotted with anti-GST monoclonal antibodies. In all lanes, the indicated proteins had co-precipitated with His-Tir I. **Lane 1:** 6 μ g GST-talin-NT2 was added first followed by addition of an equal amount of GST-vinculin tail; **Lane 2:** 6 μ g GST-vinculin tail; **Lane 3:** the order of addition was reversed; 6 μ g GST-vinculin tail followed by 6 μ g GST-talin-NT2. **Lane 4:** GST-talin-NT2 fragment is bound in the absence of the other fragment. **Lane 5:** an unrelated peptide, GST-titin A-band fragment (titin-AS), was added first, followed by GST-talin-NT2. In lanes 1–5, the amount of either the talin or vinculin fragment that binds to the His-Tir-I beads is independent of the binding of the other fragment. **Lanes 6–8:** The amount of the fragments was increased to 28 μ g. In lanes 6 and 7, the amount of talin bound by Tir I was not decreased by prior binding of an equal amount of vinculin tail. Lane 8 demonstrates that additional vinculin tail fragment could bind in the absence of GST-Talin-NT2. However, the addition of GST-Talin-NT2 could induce some of the higher amount of bound vinculin tail fragment to be released from Tir I (Lane 7). The positions of molecular weight markers are indicated on the left.

proteins are capable of binding to Tir I independently of other cellular factors and molecules.

It was surprising to find that the N-terminal region of alpha-actinin, the actin-binding region, bound to Tir I, and not the C-terminal region of the protein that harbors the integrin (and vinculin) binding domains (Figs. 3 and 4). A number of other transmembrane receptor proteins other than integrins (e.g., ADAM13, Ep-CAM, ICAMs, L-selectin, and NMDA), bind the rod part or 53-kDa part of the alpha-actinin molecule [reviewed in Ylanne et al., 2001]. The alpha-actinin binding regions of these transmembrane receptors are 7 to 31 amino acids long [Ylanne et al., 2001]. We used these different alpha-actinin binding peptide sequences in a Blast search for similar sites in Tir, but no sequence similarities were found. Alpha-actinin forms an anti-polar dimer with N-terminal regions at each end of the dimer. The location of the actin-binding and the Tir I-binding domains with respect to one another would determine if both interac-

tions could exist simultaneously. In any case, Tir-binding to alpha-actinin in host cells would occur only at the tip of the pedestal and alpha-actinin localizes along the length of the pedestal where it presumably crosslinks actin filaments.

Talin with its large size (225 kDa MW) has a number of domains that bind cytoskeletal proteins [Critchley, 2000]. Like alpha-actinin, it forms an antipolar dimer. The four talin fusion peptides used in this study were NT1, NT2, CT1, and CT2 (Fig. 2). NT1 binds actin, FAK, layalin, and beta integrin. In the His-Tir I co-precipitations and the overlays with biotinylated Tir I, all fusion peptides showed binding to Tir I (Figs. 5 and 6). Whereas, the CT2 domain was the weakest compared to the other three constructs in the biochemical binding assays, the CT2 domain yielded the only positive reaction with the yeast two-hybrid method.

The tail region of vinculin bound Tir I in the two different assays, and the N-terminal region of vinculin

only bound Tir I in coprecipitations with His-Tir I (Figs. 8 and 9). The second part of the head region of vinculin (Fig. 2) did not bind Tir I in either assay. Vinculin's ability to bind alpha-actinin and talin [Critchley, 2000] and Tir I would bring these three proteins in physical proximity where they could reinforce the attachment of Tir domains to the actin filaments located just beneath the Tir molecules. We could not detect any direct association of Tir I to actin filaments (data not shown). This suggests that Tir molecules are connected indirectly to actin filaments by other actin binding molecules like alpha-actinin, talin, and vinculin. This is similar to integrin, which binds proteins that in turn, bind actin filaments [Critchley, 2000; Sanger et al., 2000b].

It is, at first, puzzling that the three different binding assays did not always yield identical binding results. However, the presentation of the binding sites is different in the three binding assays. In one case, the His-Tir I bead-binding assay, the fusion proteins have a three-dimensional structure as they are exposed in solution to potential binding sites on Tir I. Tir I bound to beads via a His-link may be in a native conformation that approximates the kind of binding in the cell. The binding site for a particular focal adhesion protein may either be a short linear domain or may be composed of non-contiguous segments. In the biotinylated-Tir I gel overlays, the fusion proteins have been denatured and linearized over a hydrophobic nitrocellulose membrane to test their binding. Moreover, some of the hydrophobic binding sites of the fusion peptides may have been adsorbed on the nitrocellulose and thus inaccessible to the biotinylated probe. Thus, the accessibility of the binding sites of the fusion protein is very different in these two biochemical assays.

We have varied the ionic strengths and pHs of the wash solutions in the two biochemical assays and find that the domains showing binding to Tir I remained the same. Differences in domain-binding have been found in other studies using two or more assays, e.g., in a study of the binding of alpha-actinin to z-repeats of a Z-band region of titin [Young et al., 1998]. Each of the five z-repeats bound alpha-actinin in at least one of three different assays. One of the assays was a yeast two-hybrid assay. We attempted to use the yeast two hybrid assay to test the binding of the bacterial protein Tir I (bait) with each (prey) of the domains described above (Fig. 2) for alpha-actinin, talin, and vinculin. The only positive result we obtained was with the CT2 domain of talin (Fig. 7) which was also positive, but weakly, in both binding assays used in this study (Figs. 5 and 6). The yeast two-hybrid screen, like the co-precipitation assay with His-Tir I described above, depends on the interaction of the three-dimensional structures of Tir and the various focal adhesion fragments. However, these inter-

actions take place inside yeast nuclei and depend on the transport of the hybrid proteins to the nucleus from their cytoplasmic site of synthesis [Page et al., 2001]. Thus, interactions detected in biochemical assays, may not be always detected in the yeast two-hybrid screens. Similar disparities have been reported between biochemical binding assays and the yeast two-hybrid screen with other bacterial proteins [Niebuhr et al., 2000; Page et al., 2001].

We have used the technique of photobleaching to demonstrate the polarized addition of actin at the pedestal tip and the subsequent flow of actin molecules from the tips of pedestals to the base at the cell body where actin disassembly is completed [Shaner et al., 2001]. If the three proteins are bound to Tir I and actin in the infected cell, there would need to be a momentary release of the Tir-attached, actin-binding proteins (alpha-actinin, talin, and vinculin) either from the actin filaments undergoing actin monomer incorporation in this area, or from Tir. Future work will be needed to distinguish between these two possibilities. In conclusion, the results of this study support the interpretation advanced by Freeman et al. [2000] that the pedestals are a composite of focal adhesions [Goosney et al. 2001] and microvilli. The extracellular substrate, the intimin coated EPEC, is connected to the transmembrane protein, Tir, which in turn has its cytoplasmic domains connected to focal adhesion proteins like alpha-actinin, talin, and vinculin.

ACKNOWLEDGMENTS

We thank Dr. Nancy Freeman for her critical suggestions on improving the manuscript. This work was supported by a grant from the United States Department of Agriculture (Research Institute Competitive Grants Program of the USDA, agreement 99-35204-7864 to J. M. S.)

REFERENCES

- Cantarelli VV, Takahashi A, Yanagihara I, Akeda Y, Imura K, Kodama T, Kono G, Sato Y, Honda T. 2001. Talin, a host cell protein, interacts directly with the translocated intimin receptor, Tir, of enteropathogenic *Escherichia coli*, and is essential for pedestal formation. *Cell Microbiol* 3:745-751.
- Celli J, Deng W, Finlay BB. 2000. Enteropathogenic *Escherichia coli* (EPEC) attachment to epithelial cells: exploiting the host cell cytoskeleton from the outside. *Cell Microbiol* 2:1-9.
- Critchley DR. 2000. Focal adhesions: the cytoskeletal connection. *Curr Opin Cell Biol* 12:133-139.
- de Grado M, Abe A, Gauthier A, Steele-Mortimer O, DeVinney R, Finlay BB. 1999. Identification of the intimin-binding domain of Tir of enteropathogenic *Escherichia coli*. *Cell Microbiol* 1:7-17.
- DeVinney R, Stein M, Reinscheid D, Abe A, Ruschkowski S, Finlay BB. 1999. Enterohemorrhagic *Escherichia coli* O157:H7 pro-

- duces Tir, which is translocated to the host cell membrane but is not tyrosine phosphorylated. *Infect Immun* 67:2389–2398.
- DeVinney R, Puente JL, Gauthier A, Goosney D, Finlay BB. 2001. Enterohaemorrhagic and enteropathogenic *Escherichia coli* use a different Tir-based mechanism for pedestal formation. *Mol Microbiol* 41:1445–1458.
- Dold F, Sanger JM, Sanger JW. 1994. Intact alpha-actinin molecules are needed for both the assembly of actin into the tails and the locomotion of *Listeria monocytogenes* inside infected cells. *Cell Motil Cytoskeleton* 28:97–107.
- Donnenberg MS, Tacket CO, James SP, Losonsky G, Nataro JP, Wasserman SS, Kaper JB, Levine MM. 1993. Role of the *eaeA* gene in experimental enteropathogenic *Escherichia coli* infection. *J Clin Infect* 92:1412–1417.
- Freeman NL, Zurawski DV, Chowrashi P, Ayoob JC, Huang L, Mittal B, Sanger JM, Sanger JW. 2000. Interaction of the enteropathogenic *Escherichia coli* protein, translocated intimin receptor (Tir), with focal adhesion proteins. *Cell Motil Cytoskeleton* 47:307–318.
- Fukui H, Sueyoshi M, Haritani M, Nakazawa M, Naitoh S, Tani H, Uda Y. 1995. Natural infection with attaching and effacing *Escherichia coli* (O 103:H-) in chicks. *Avian Dis* 39:912–918.
- Goosney DL, DeVinney R, Finlay BB. 2001. Recruitment of cytoskeletal and signaling proteins to enteropathogenic and enterohemorrhagic *Escherichia coli* pedestals. *Infect Immun* 69:3315–3322.
- Goosney DL, DeVinney R, Pfuetzner RA, Frey EA, Strynadka NC, Finlay BB. 2000a. Enteropathogenic *E. coli* translocated intimin receptor, Tir, interacts directly with alpha-actinin. *Curr Biol* 10:735–738.
- Goosney DL, Gruenheid S, Finlay BB. 2000b. Gut feelings: enteropathogenic *E. coli* (EPEC) interactions with the host. 2000. *Annu Rev Cell Dev Biol* 16:173–189.
- Gruenheid S, DeVinney R, Bladt F, Goosney D, Gelkop S, Gish GD, Pawson T, Finlay BB. 2001. Enteropathogenic *E. coli* Tir binds Nck to initiate actin pedestal formation in host cells. *Nat Cell Biol* 3:856–859.
- Hecht G. 1999. Innate mechanisms of epithelial host defense: spotlight on intestine. *Am J Physiol* 277:C351–C358.
- Hock RS, Sanger JM, Sanger JW. 1989. Talin dynamics in living microinjected nonmuscle cells. *Cell Motil Cytoskeleton* 14:271–287.
- Hooper LV, Bry L, Falk PG, Gordon JI. 1998. Host-microbial symbiosis in the mammalian intestine: exploring an internal ecosystem. *BioEssays* 20:336–343.
- Levine MM. 1987. *Escherichia coli* that cause diarrhea: enterotoxigenic, enteropathogenic, enteroinvasive, enterohemorrhagic and enteroadherent. *J Infect Dis* 155:377–389.
- Luo Y, Frey EA, Pfuetzner RA, Creagh AL, Knoechel DG, Haynes CA, Finlay BB, Strynadka NC. 2000. Crystal structure of enteropathogenic *Escherichia coli* intimin-receptor complex. *Nature* 405:1073–1077.
- Marches O, Nougayrede J-P, Boullier S, Mainl J, Charlier G, Raymond I, Pohl P, Boury M, DeRycke J, Milon A, Oswald E. 2000. Role of Tir and intimin in the virulence of rabbit enteropathogenic *Escherichia coli* serotype O103:H2. *Infect Immun* 68:2171–2182.
- Nataro JP, Kaper JB. 1998. Diarrheagenic *Escherichia coli*. *Clin Micro Rev* 11:142–201.
- Neutra MR. 1988. The gastrointestinal tract. In: Weiss L, editor. *Cell and tissue biology: a textbook of histology*. Baltimore: Urban and Schwarzenberg, p 641–683.
- Niebuhr K, Jouihri N, Allaoui A, Gounon P, Sansonetti PJ, Parsot C. 2000. IpgD, a protein secreted by the type III secretion machinery of *Shigella Flexneri*, is chaperoned by IpgE and implicated in early focus formation. *Mol Microbiol* 38:8–19.
- Page AL, Fromont-Racine M, Sansonetti P, Legrain P, Parsot C. 2001. Characterization of the interaction partners of secreted proteins and chaperones of *Shigella flexneri*. *Mol Microbiol* 42:1133–1145.
- Rees DJG, Ades SE, Singer SJ, Hynes RO. 1990. Sequence and domain structure of talin. *Nature* 347:685–689.
- Sanger JM, Chang R, Ashton F, Kaper JB, Sanger JW. 1996. Novel form of actin-based motility transports bacteria on the surfaces of infected cells. *Cell Motil Cytoskeleton* 34:279–287.
- Sanger JM, Danowski BA, Sanger JW. 2000a. Microinjection of fluorescently labeled alpha-actinin into living cells. In: Tuan RS, Lo CW, editors. *Methods in molecular biology: developmental biology protocols*, vol. III. Totowa, NJ: Humana Press, p 449–456.
- Sanger JW, Ayoob JC, Chowrashi P, Zurawski D, Sanger JM. 2000b. Assembly of myofibrils in cardiac muscle cells. *Adv Exp Med Biol* 481:89–102.
- Savage DA. 1977. Microbial ecology of the gastrointestinal tract. *Ann Rev Microbiol* 31:107–133.
- Shaner NC, Sanger JW, Sanger JM. 2001. A model to describe actin dynamics beneath EPEC and EHEC in infected cells. *Mol Biol Cell* 12:424a.
- Vallance, BA, Finlay, BB. 2000. Exploitation of host cells by enteropathogenic *Escherichia coli*. *Proc Natl Acad Sci USA* 97:8799–8806.
- Ylanne J, Scheffzek K, Young P, Saraste M. 2001. Crystal structure of the alpha-actinin rod reveals an extensive torsional twist. *Structure* 9:597–604.
- Young P, Ferguson C, Banuelos S, Gautel M. 1998. Molecular structure of the sarcomeric Z-disk: two types of titin interactions lead to an asymmetrical sorting of alpha-actinin. *EMBO J* 17:1614–1624.